



# A study on optical, spectroscopic and structural properties of copper-doped calcium lithium borate glasses

Ismail Rammadhan Mohammed<sup>1</sup>

Received: 25 May 2020 / Accepted: 31 July 2020 / Published online: 16 August 2020  
© The Optical Society of India 2020

**Abstract** In this work, the physical properties of calcium lithium borate glasses are investigated upon the inclusion of  $\text{Cu}^{+2}$  ion dopant. UV–Vis–NIR, photoluminescence, FTIR, and XRD techniques were, respectively, used in this study. From the optical absorption response of the samples, direct and indirect energy band gaps were calculated and they were found to be in the ranges of 3.57–3.28 eV and 3.78–3.6 eV, respectively. Results showed that the refractive index was increased from 2.258 to 2.326 with the increase in  $\text{Cu}_2\text{O}$  concentration. Also, three main emission bands were observed in the luminescence spectra at around 399, 483, and 575 nm, which are correlated with the change in the copper concentration. Results of the FTIR spectroscopy showed various peaks in the ranges of  $1383\text{--}1415\text{ cm}^{-1}$  and  $1062\text{--}1076\text{ cm}^{-1}$ , which can be attributed to the trigonal and tetrahedral stretching vibrations of  $\text{BO}_3$  and  $\text{BO}_4$  units.

**Keyword** Optical properties · FTIR · Photoluminescence · Copper impurities · Physical properties

## Introduction

In recent years, glasses doped with transition metal ions have attracted a great deal of attention due to their unique properties such as hardness, good strength, transparency, excellent corrosion resistance, and photoconducting properties [1]. The properties of glasses are mainly determined

by the degree of local order/disorder, through which information about the local structure can be retrieved. UV–VIS and FTIR spectroscopies are very useful to provide valuable information related to the local symmetry, nature of chemical bonds and other structural properties of glasses [2].

Boric oxide is one of the most common glass-forming oxides and has been incorporated with various types of modifier metal oxide to attain the desired physical and chemical properties [3]. Boric oxide,  $\text{B}_2\text{O}_3$  is generally interesting amorphous materials because of their structures and physical properties. In these glasses, two groups of bands are obtained: (a) due to trigonal  $\text{BO}_3$  units and (b) due to tetrahedral  $\text{BO}_4$  units. By the addition of transition metal ions to the borate glasses, they would show specific physical properties [4, 5]. Pure borate glasses are not of practical use because of their high hygroscopic nature and weak glow peak at low temperatures so they can be improved with the addition of alkali metals to get good physical properties. They are also studied as dosimetric materials which are ideal materials for the environment [6].

The transition metal-doped glasses are mainly used for applications in electrochemical, electronic, and optoelectronic devices. Optical absorption of some transition metal ions also gives rise to ligand field absorption energies [7]. On the other hand, the small quantity of transition metal oxide when added to glasses like borate strongly influences the physical properties. Copper oxide is one of the transition metal oxides which are used in industries for colored glasses. Copper exists in two stable ionic states, the divalent  $\text{Cu}^{2+}$  and monovalent  $\text{Cu}^+$  ions [8]. The cuprous ion ( $\text{Cu}^+$ ) does not produce color, but  $\text{Cu}^{2+}$  ion-doped glasses are important due to their optical stability [9].

Thus, the purpose and objective of the current study are to investigate the effect of copper ions concentration on

✉ Ismail Rammadhan Mohammed  
ismail.ammadhan@koyauniversity.org

<sup>1</sup> Department of Physics, Faculty of Sciences and Health, Koya University, Koya KOY45, Erbil, Kurdistan Region, Iraq

optical, spectroscopic, and structural properties of calcium lithium borate glasses. Additionally, the current results are in good agreement with other studies and confirm the suitability of these glasses in the broadband optical fiber and other optical devices.

## Methods

### Experimental procedures

Compounds in powder form in mol% were utilized to obtain the glass samples with the composition of (1) (80H<sub>3</sub>BO<sub>3</sub>–10CaCO<sub>3</sub>–10Li<sub>2</sub>CO<sub>3</sub>) called as Glass S<sub>0</sub> (without Cu<sub>2</sub>O); (2) (80-*x*)H<sub>3</sub>BO<sub>3</sub>–10CaCO<sub>3</sub>–10Li<sub>2</sub>CO<sub>3</sub>–*x*Cu<sub>2</sub>O system, where *x* = 0.01, 0.02, 0.04, 0.06 and 0.08%; these glasses are classified as S<sub>1</sub>, S<sub>2</sub>, S<sub>3</sub>, S<sub>4</sub>, and S<sub>5</sub>, respectively. The details of techniques adopted for the preparation of the samples were reported before [10]. The compositions of the prepared samples are portrayed in Table 1.

Powder samples of glasses were analyzed in computer-assisted X-ray (Cu Kα) of wavelength λ = 1.54 Å as radiation that was running at 40 kV and 30 mA at room temperature. The test was conducted out in the range from 2θ = 5°–80° utilizing Siemens diffractometer D6000.

The optical absorption spectra in the visible and near-ultraviolet region were measured at room temperature by using Shimadzu (UV–3101PC) UV–Vis–NIR scanning spectrophotometer in the wavelength range from 200 to 1800 nm. By using the Perkin Elmer LS55 luminescence spectrophotometer, the photoluminescence spectrum was measured.

FTIR transmission spectra measurements are performed on thin disks formed by mixing the powder from the glass sample with potassium bromide (KBr) in an agate mortar in the ratio of 1:100 mg. The mixture was then pressed at 120 MPa for one minute to obtain a transparent disk.

**Table 1** Glass samples code and their compositions (mol %)

Sample code	Composition (mole %)			
	CaCO <sub>3</sub>	Li <sub>2</sub> CO <sub>3</sub>	H <sub>3</sub> BO <sub>3</sub>	Cu <sub>2</sub> O
S <sub>0</sub>	10	10	80.0	0.0
S <sub>1</sub>	10	10	79.99	0.01
S <sub>2</sub>	10	10	79.98	0.02
S <sub>3</sub>	10	10	79.96	0.04
S <sub>4</sub>	10	10	79.94	0.06
S <sub>5</sub>	10	10	79.92	0.08

## Results and discussion

### X-ray diffraction spectra

The X-ray diffraction (XRD) technique is a modern and nondestructive testing method used to determine the crystallographic structure and amorphous state of materials. The prepared glasses were smashed into fine powders using mortar and pellet. Figure 1 shows the typical X-ray diffraction pattern for S<sub>2</sub> glass. The truancy of any sharp peaks confirms the amorphous nature of the glass [11].

### UV–Vis absorption spectra

The optical energy gap was determined for all the samples based on their UV absorption spectra. For this purpose, plots of (αE)<sup>*n*</sup> as a function of photon energy (*E*) were produced and the optical energy gap was calculated using the Tauc’s equation [12]:

$$\alpha E = a_o [E - E_g]^n \tag{1}$$

where E<sub>g</sub> is the energy gap, α is the absorption coefficient, E is photon energy, and a<sub>o</sub> is an energy-independent constant. The value of exponent *n* in the equation defines the nature of the electronic transition between the valence and conduction bands. The value of *n* is 1/2 and 2 for direct and indirect transitions, respectively. The value of the absorption coefficient can also be determined using the following formula:

$$\alpha = 2.303 \left( \frac{A}{d} \right) \tag{2}$$

where *d* is the thickness of the sample and *A* is the absorption. Figure 2a, b shows the ultraviolet absorption edge and corresponding (αE)<sup>*n*</sup> versus photon energy (*E*) for CLB:Cu<sub>2</sub>O-doped glass samples. From this plot, the respective values of the optical energy gap (E<sub>g</sub>) can be obtained by extrapolating the linear region of the curve to the energy axis at (αE)<sup>*n*</sup> → 0. Results showed that the

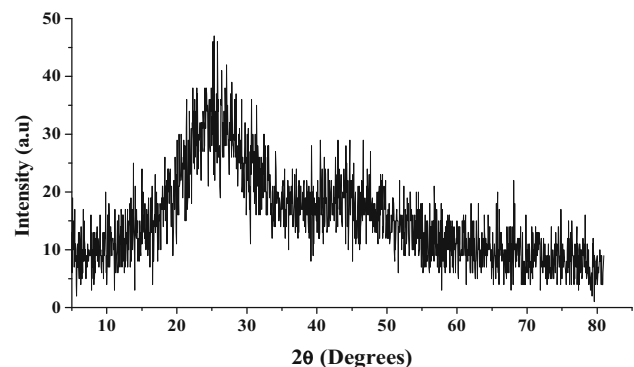


**Fig. 1** X-ray diffraction patterns for the S<sub>2</sub> sample

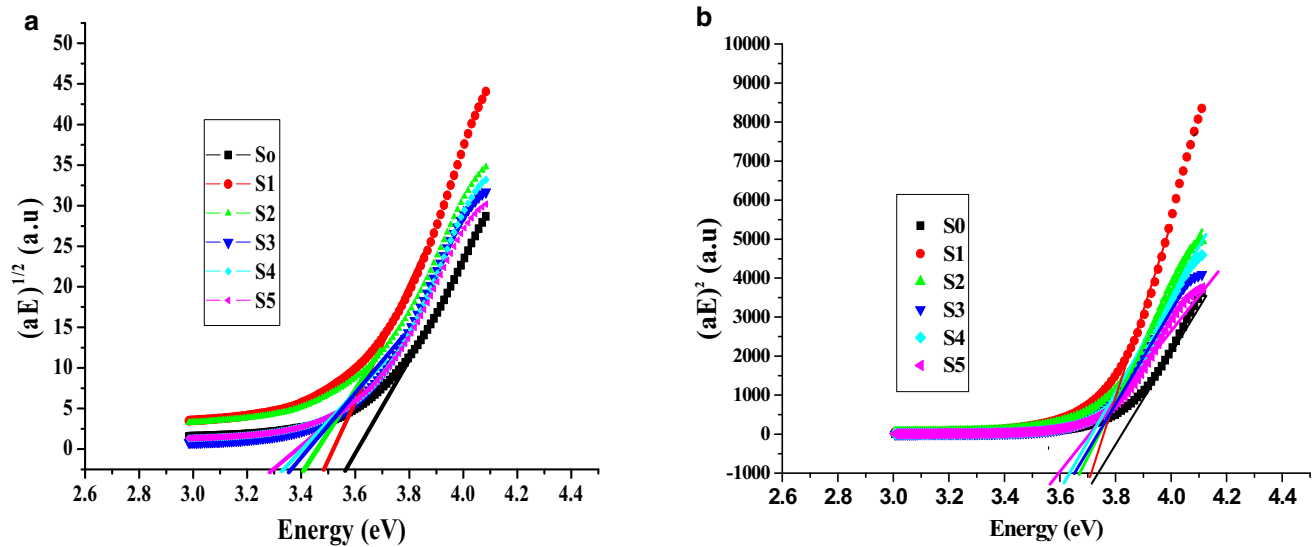


**Fig. 2** Plot of  $(\alpha hv)^n$  versus photon energy for CLB:Cu<sub>2</sub>O glasses **a**  $n = 1/2$  for direct transition, **b**  $n = 2$  for indirect transition

value of  $E_g$  is decreased with the increase in Cu<sub>2</sub>O concentrations (see Table 3).

When photon energy in the region of optical absorption is less than the band gap energy, this region is referred to as the Urbach tail region and the relation between optical absorption and photon energy is exponential. The Urbach energy can be calculated by used the following relation [13]:

$$\alpha = a_0 \exp\left(\frac{hv}{E_u}\right) \quad (3)$$

where  $E_u$  is the Urbach's energy representing the width of the localized state tails in the band gap. The values of  $E_u$  are obtained by taking the reciprocals of the slopes of the linear portion in the lower photon energy region of  $\ln \alpha$

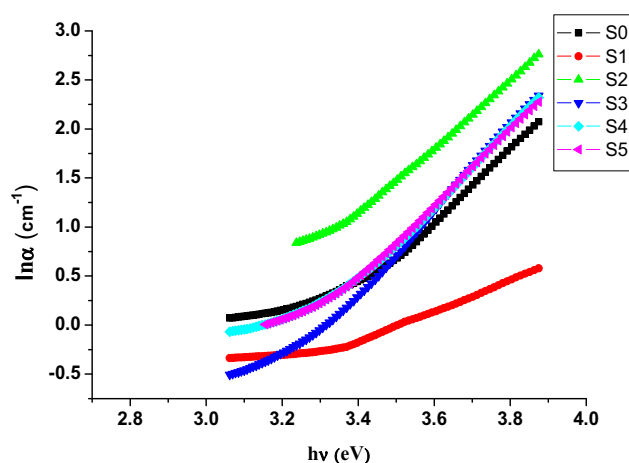


**Fig. 3** Plot of  $\ln \alpha$  versus  $hv$  for CLB glass doped with different mol% of Cu<sub>2</sub>O

versus  $hv$  as shown in Fig. 3. The values of  $E_u$  for all samples are given in Table 3.

Figure 4 shows the UV–Vis–NIR absorption spectra for all the prepared samples. It can be seen from the UV spectra of the Cu<sup>2+</sup> ion-doped glasses that there is a transmission window in the wavelength range from 440 to 500 nm. This is a very interesting range for these borate glasses, making them viable for the application of selective absorption radiations. The shift of the ultraviolet absorption band to longer wavelengths corresponds to transitions from the nonbridge of oxygen (NBO) which binds an excited electron less tightly than the bridging oxygen [14].

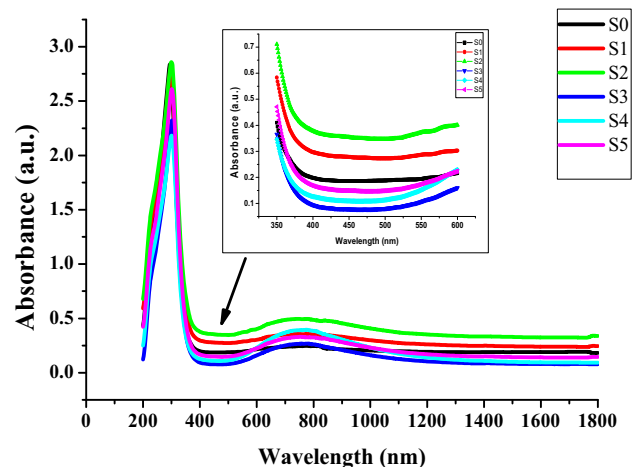


**Fig. 4** UV–Vis–NIR absorption spectra of CLB glass doped with different mol% of Cu<sub>2</sub>O

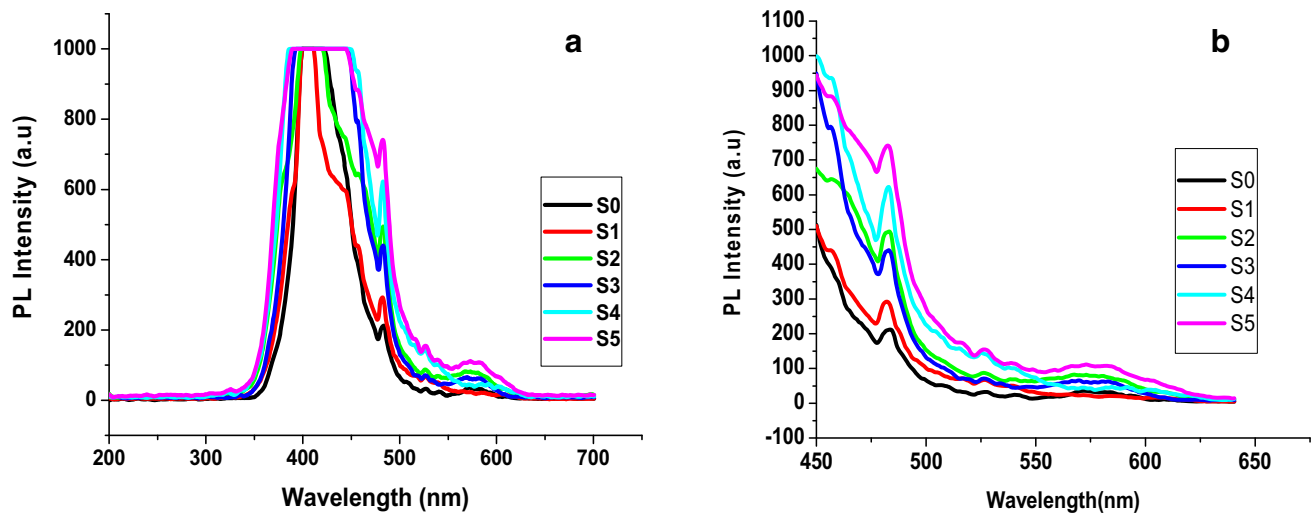


**Fig. 5** PL spectra of CLB:Cu samples

### Photoluminescence spectra

The PL spectra of CLB:Cu glasses are shown in Fig. 5a, b; the spectra include three main emission bands: The strong emission peak wavelength of 399 nm band is slightly shifted toward a higher wavelength 445 nm. The intensity of all peaks in this band unchanged with the increase in  $\text{Cu}_2\text{O}$  content in the host glass. The second band was observed at around 483 nm, and the intensity increased gradually with the increase in  $\text{Cu}_2\text{O}$ -doped contents. The last emission band at around 573 nm is slightly shifted toward a higher wavelength of 580 nm with a slight increase in intensity upon different concentrations of  $\text{Cu}^{2+}$  ions. Figure 5b clearly shows that the PL intensity is quenched with increasing the  $\text{Cu}^{2+}$  ion concentration. Then, it increased and decreased again such that sample S5 revealed the maximum PL intensity. This decrease in PL intensity (sample S3) is mainly attributed to the  $\text{Cu}^{2+}$  ions concentration quenching effects and the instability of the excited ions at the most upper level.

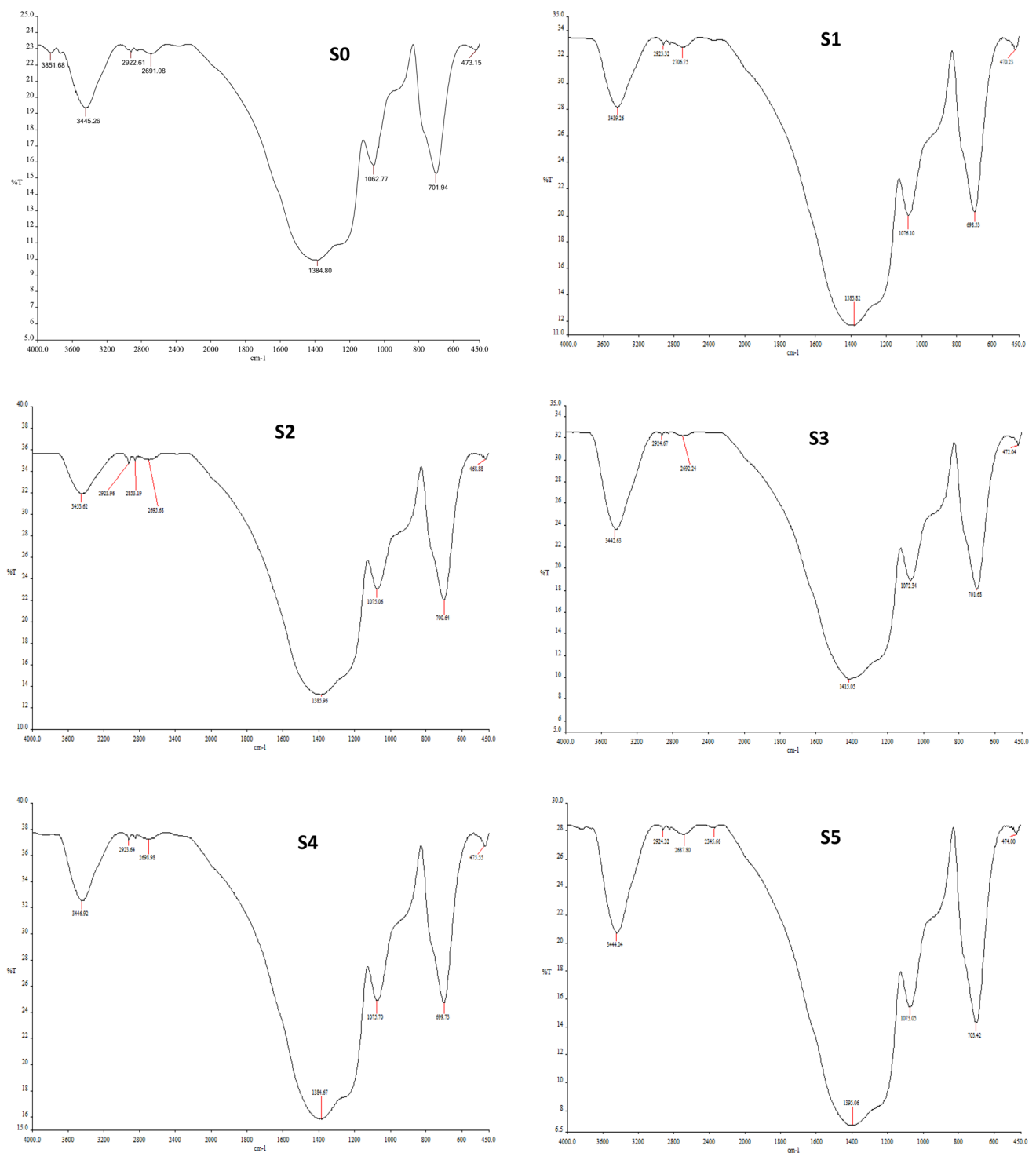
### FTIR spectroscopy

Figure 6 shows the FTIR transmittance spectra of as-prepared glasses in the wave number region ( $400\text{--}4000\text{ cm}^{-1}$ ) at room temperature. The bands observed from the FTIR spectra and their corresponding assignments are summarized in Table 2. The vibrational modes of the borate network are mainly active in three infrared spectral regions, which are similar to those reported by other researchers [15]. The first band occurring at  $1200\text{--}1600\text{ cm}^{-1}$  is due to the asymmetric stretching relaxation of the B–O band of trigonal  $\text{BO}_3$  units. The second band between  $800$  and  $1200\text{ cm}^{-1}$  is due to the B–O bond stretching of the

tetrahedral  $\text{BO}_4$  units, and the third group observed around  $700\text{ m}^{-1}$  is due to bending of B–O–B linkages in the borate network. Furthermore, the band from  $2400$  to  $4000\text{ cm}^{-1}$  is due to the O–H vibration of water group [15–17].

A weak band in the region of ( $468\text{--}476\text{ cm}^{-1}$ ) was formed due to the bending vibrations of various borate arrangements, vibrations of calcium, lithium cations through glass network [6, 18], which is due to the specific vibrations of Cu–O, while the band in a range of ( $698\text{--}705\text{ cm}^{-1}$ ) is attributed to B–O–B bending vibrations of borate network [19–21]. The band at ( $1062\text{--}1076\text{ cm}^{-1}$ ) is assigned to the stretching vibrations of B–O bonds in  $\text{BO}_4$  units from tri-, tetra-, and penta-borate groups [19]. The band at ( $1383\text{--}1415\text{ cm}^{-1}$ ) is due to the stretching vibrations of the B–O of triangle ( $\text{BO}_3$ ) units in meta-borates, pyro-borates, and ortho-borates [22, 23]. The bands ( $3439\text{--}3855\text{ cm}^{-1}$ ) are attributed to the symmetric stretching of O–H groups (H–O–H) [24]. In the study, it was noticed that the IR intensity of all the peaks is increased when the concentration of  $\text{Cu}_2\text{O}$  is increased. The enhancement of peak intensity indicates the increase in bond vibration and the shift toward higher wave number which is due to the increase in the bond length of B–O groups and the formation of  $\text{BO}_4$  units [25, 26].

From the FTIR spectra, already one can notice that the addition of  $\text{Cu}^{2+}$  in CLB has contributed to modifying the glass network. It has been perceived that  $\text{Cu}^{2+}$  content helps in converting ( $\text{BO}_3$ ) groups to ( $\text{BO}_4$ ) units. This reveals that  $\text{Cu}^{2+}$  ions have a dominant role in the CLB glass system.



**Fig. 6** FTIR spectra of all samples

## Physical properties

### *Density and molar volume*

By applying Archimedes principle, the mass of the prepared glass samples is measured in air and in liquid, the

density ( $\rho$ ) of the prepared glass samples and molar volume [ $V_M$  ( $\text{cm}^3/\text{mol}$ )] have been calculated at room temperature with toluene as the immersion liquid ( $\rho_o = 0.8669 \text{ g/cm}^3$ ) on a single-pan electronic balance with an accuracy of 0.001 mg using the following formula:

**Table 2** FTIR peaks position of prepared glass samples

Wave numbers (cm <sup>-1</sup> )	Band assignments
468–476	Angles modification of B–O–B linkages
698–705	BO <sub>3</sub> –O–BO <sub>4</sub> bending vibrations
1062–1076	B–O (stretching of tetrahedral BO <sub>4</sub> bond)
1383–1415	B–O (stretching of trigonal BO <sub>3</sub> bond)
2687–2925	Hydrogen bending
3439–3855	O–H (H <sub>2</sub> O bond)

$$\rho = \frac{W_{\text{air}}}{W_{\text{air}} - W_L} \rho_0 \tag{4}$$

$$V_M = \frac{\sum x_i M_i}{\rho} \tag{5}$$

where  $W_{\text{air}}$  is the mass in air,  $W_L$  is the mass in toluene,  $x_i$  is the molar fraction and  $M_i$  is the molecular weight of the  $i$ th component of the glass. The density is found to decrease continuously from 2.1246 to 2.1056 g cm<sup>-3</sup> with the increase in Cu<sub>2</sub>O-doped concentration (see Table 3). This decrease is majorly attributed to the following mechanisms:

- (1) Conversion of BO<sub>3</sub> triangles into BO<sub>4</sub> tetrahedral,
- (2) enhancement of molecular mass of the glass due to insertion of the higher atomic weight of calcium, and (3) increase in the oxygen–boron ratio because of the increase in Cu<sub>2</sub>O-doped concentration. Another indication of the glass structure compactness reduction is the simultaneous increase in molar volume (30.25–30.56 cm<sup>3</sup>/mol). This increase is ascribed to the increase in bond length or

interatomic spacing among the atoms of the glass network which causes compaction of structure [27, 28]. The average boron–boron separation  $\langle d_{B-B} \rangle$  is calculated to confirm the modification of the glass network due to the presence of copper oxide. Thus, the volume  $V_m^B$  corresponding to the volume that contains one mole of boron within the given structure is defined as [29]:

$$V_m^B = \frac{V_m}{2(1 - x_i)} \tag{6}$$

where  $V_m$  is molar volume,  $x_i$  molar fraction of B<sub>2</sub>O<sub>3</sub>

$$\langle d_{B-B} \rangle = \left( \frac{V_m^B}{N_A} \right)^{1/3} \tag{7}$$

where  $N_A$  is Avogadro number. The value  $\langle d_{B-B} \rangle$  slightly increased with increase in Cu<sub>2</sub>O contents, and the measured values of  $\langle d_{B-B} \rangle$  are recorded in Table 3.

*Refractive index, molar refraction and molar polarizability*

The values of the optical band gap ( $E_g$ ) (indirect allowed) consequently lead to refractive index results. The refractive index ( $n$ ) of each sample is calculated using the relation [29, 30]

$$\frac{n^2 - 1}{n^2 + 2} = 1 - \sqrt{\frac{E_g}{20}} \tag{8}$$

From the measured values of  $n$  and molar volume ( $V_M$ ), molar refractivity ( $R_M$ ) and molar polarizability ( $\alpha_m$ ) of the glasses have been calculated using the following relations [29, 31, 32]:

**Table 3** Measured optical properties, physical properties and inter-nuclear properties for all samples

Properties	Doped Cu <sub>2</sub> O (mol %)					
	0.0	0.01	0.02	0.04	0.06	0.08
Direct band gap energy, $E_g$ (eV)	3.57	3.49	3.41	3.38	3.33	3.28
Indirect band gap energy, $E_g$ (eV)	3.78	3.74	3.69	3.67	3.63	3.6
Urbach energy, $E_u$ (eV)	0.3048	0.3105	0.3135	0.3175	0.3194	0.3115
Density, $\rho$ (g/cm <sup>3</sup> )	2.1246	2.1241	2.1203	2.1193	2.1182	2.1056
Molar volume, $V_m$ (cm <sup>3</sup> /mol)	30.259	30.270	30.328	30.349	30.372	30.56
Refractive index, $n$	2.258	2.276	2.295	2.302	2.313	2.326
Molar refractivity, $R_m$ (cm <sup>3</sup> )	17.471	17.622	17.808	17.875	17.975	18.188
Molecular weight, $M_w$	64.29	64.297	64.304	64.319	64.334	64.349
Average boron–boron separation, ( $\langle d_{B-B} \rangle$ nm)	–	0.36217	0.36279	0.36322	0.36335	0.3649
Molar polarizability, $\alpha_m$ (Å <sup>3</sup> )	6.925	6.985	7.059	7.086	7.125	7.21
Cu <sup>2+</sup> ion concentration, $N$ (ion/cm <sup>3</sup> ) × 10 <sup>20</sup>	–	1.988	3.97	7.934	11.892	15.758
Inter-nuclear distance, $r_i$ (Å)	–	8.5661	6.803	5.401	4.719	4.296
Polaron radius, $r_p$ (Å)	–	6.9031	5.4824	4.3524	3.8031	3.4625
Field strength, $F$ (cm <sup>-2</sup> ) × 10 <sup>15</sup>	–	6.085	9.648	15.308	20.049	24.188

$$R_M = \frac{n^2 - 1}{n^2 + 2} V_M \quad (9)$$

$$\alpha_m = \left( \frac{3}{4\pi N_A} \right) R_M \quad (10)$$

The measured values of refractive index ( $n$ ), molar volume ( $V_M$ ), molar refractivity ( $R_M$ ) and molar polarizability ( $\alpha_m$ ) are depicted in Table 3. Figure 7 shows that the refractive index and molar refractivity increase with the increase in  $\text{Cu}_2\text{O}$  concentration. This increase is mainly due to the creation of nonbridging oxygen atoms as a result of breakage of glass network structures and subsequent enhancement in the polarizability [33].

### Internuclear properties

#### *Ion concentration*

The ions concentration inside the current samples can be calculated by using the formula [34]:

$$N = \frac{\text{mole\% of doped} \times \rho \times N_A}{\text{Average molecular weight of glass}} \text{ (Ion cm}^{-1}\text{)} \quad (11)$$

#### *Polaron radius, internuclear distance and field strength*

Other related internuclear properties such as polaron radius, internuclear distance, and field strength can be calculated after the determination of ion concentration by using the following equations [35]:

$$\text{Polaron radius } r_p (\text{\AA}) = \frac{1}{2} \left( \frac{\pi}{6N} \right)^{\frac{1}{3}} \quad (12)$$

$$\text{Inter-nuclear distance } r_i (\text{\AA}) = \left( \frac{1}{N} \right)^{\frac{1}{3}} \quad (13)$$

The field strength is expressed as,

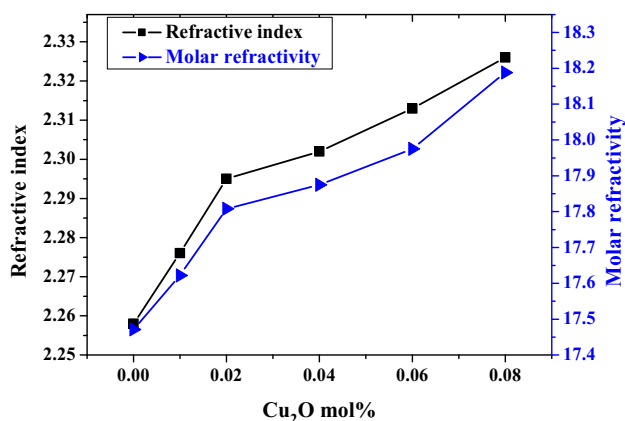


**Fig. 7** Variation in refractive index and molar refraction of CLB:Cu glass

$$F = \left( \frac{Z}{r_p^2} \right) \quad (14)$$

The measured values of ions concentration ( $N$ ), polaron radius ( $r_p$ ), internuclear distance ( $r_i$ ) and field strength ( $F$ ) are summarized in Table 3.

### Conclusion

From the spectroscopic investigations of (CLB:Cu) glasses, the following conclusions are drawn:

1. The analysis of optical absorption data reveals that the optical band gap values are decreased with an increase in  $\text{Cu}_2\text{O}$  concentration.
2. The UV–Vis absorption spectra of glasses show that in the copper oxide-doped glasses, there is the transmission window range from 440 to 500 nm.
3. Test dopant  $\text{Cu}^{2+}$  ion concentration variation influences the physical properties such as glass density, molar volume, molar refractivity, polaron radius, internuclear distance, molar polarizability ( $\alpha_m$ ) and field strength.
4. The photoluminescence spectra revealed three excitation bands at around 399 nm, 483 nm and 575 nm.
5. The FTIR studies revealed that the network structures of the studied glasses were related to the characteristic borate bonds, especially  $\text{BO}_3$  and  $\text{BO}_4$  units.

**Acknowledgments** I would like to thank the Research Center for Studies and their Promising Technologies, Koya University, Koya, Erbil, Iraq.

### References

1. M. Pal, B. Roy, M. Pal, Structural characterization of borate glasses containing zinc and manganese oxides. *J. Mod. Phys.* **2**, 1062–1066 (2011)
2. S. Shailajha, K. Geetha, P. Vasantharani, S.P. Sheik Abdul Kadhar, Effects of copper on the preparation and characterization of Na-Ca-P borate glasses. *Spectrochim. Acta Part Mol. Biomol. Spectrosc.* **138**, 846–856 (2015)
3. Y. Tetsuji, N. Kunimine, S. Shibata, M. Yamane, Structural investigation of sodium borate glasses and melts by raman spectroscopy, II,—conversion between  $\text{BO}_4$  and  $\text{BO}_2\text{O}$ —units at high temperature. *J. Non-Cryst. Solids.* **321**, 147–156 (2003)
4. A.T. Madej, K.C. Kowalska, M. Laczka, The effect of silicate network modifiers on colour and electron spectra of transition metal ions. *Opt. Mater.* **32**, 1456–1462 (2010)
5. P.V. Reddy, C.L. Kanth, V.P. Kumar, N. Veeraiah, P. Kistaiah, Optical and thermoluminescence properties of  $\text{R}_2\text{O}$ –RF– $\text{B}_2\text{O}_3$  glass systems doped with MnO. *J. Non-Cryst. Solids.* **351**, 3752–3759 (2005)
6. A. Haydar, W. Husain, R. Hussin, H. Ali, Y. Alajerami, M.A. Saeed, Thermoluminescence properties of the Cu-doped lithium

- potassium borate glass. *Appl. Radiat. Isot.* **90**, 35–39 (2014). <https://doi.org/10.1016/j.apradiso.2014.01.012>
7. N.S. Rao, M. Purnima, S. Bale, S.K. Kumar, S. Rahman, Spectroscopic investigations of  $\text{Cu}^{2+}$  in  $\text{Li}_2\text{O}-\text{Na}_2\text{O}-\text{B}_2\text{O}_3-\text{Bi}_2\text{O}_3$  glasses. *Bull. Mater. Sci.* **29**, 365–370 (2006)
  8. H. El-Batal, Z. El-Mandouh, H. Zayed, S. Marzouk, G. El-Komy, A. Hosny, Optical and infrared properties of lithium diborate glasses doped with copper oxide. *J. Indian Pure Phys.* **50**, 398–404 (2012)
  9. H.A. ElBatal, A.M. Abdelghany, I.S. Ali, Optical and FTIR studies of CuO-doped lead borate glasses and effect of gamma-irradiation. *J. Non-Cryst. Solids.* **358**, 820–825 (2012)
  10. I. Rammadhan, S. Taha, H. Wagiran, Thermoluminescence characteristics of  $\text{Cu}_2\text{O}$  doped Calcium Lithium borate glass irradiated with the cobalt-60 gamma rays. *J. Lumin.* **186**, 117–122 (2017)
  11. N.A. Zarifah, M.K. Halimah, M. Hashim, B.Z. Azmi, W.M. Daud, Magnetic behaviour of  $(\text{Fe}_2\text{O}_3)_x(\text{TeO}_2)_{1-x}$  glass system due to iron oxide. *Chalcogenide Letters* **7**, 565–571 (2010)
  12. E.A. Davis, N.F. Mott, Conduction in non-crystalline systems V. *Philos. Mag.* **22**, 903–922 (1970). <https://doi.org/10.1080/14786437008221061>
  13. F.F. Muhammad, M.Y. Yahya, F. Aziz, M.A. Rasheed, K. Sulaiman, Tuning the extinction coefficient, refractive index, dielectric constant and optical conductivity of Gaq3 films for the application of OLED displays technology. *J. Mater. Sci. Mater. Electron.* **28**, 14777–14786 (2017). <https://doi.org/10.1007/s10854-017-7347-y>
  14. J.E. Shelby, *Introduction to Glass Science and Technology*, 2nd edn. (The Royal Society of Chemistry, Cambridge, 2005). ISBN: 978-1-84755-116-0
  15. E.I. Kamitsos, M.A. Karakassides, G.D. Chryssikos, Vibrational-spectra of magnesium–sodium–borate glasses. 2. Raman and midinfrared investigation of the network structure. *J. Phys. Chem.* **91**, 1073–1079 (1987). <https://doi.org/10.1021/j100289a014>
  16. J. Krogh-Moe, the structure of vitreous and liquid boron oxide. *J. Non-Cryst. Solids.* **1**, 269–284 (1969). [https://doi.org/10.1016/0022-3093\(69\)90025-8](https://doi.org/10.1016/0022-3093(69)90025-8)
  17. L. Stoch, M. Sroda, Infrared spectroscopy in the investigation of oxide glasses structure. *J. Mol. Struct.* **511**, 77–84 (1999). [https://doi.org/10.1016/S0022-2860\(99\)00146-5](https://doi.org/10.1016/S0022-2860(99)00146-5)
  18. G. Padmaja, P. Kistaiah, Infrared and Raman spectroscopic studies on alkali borate glasses: evidence of mixed alkali effect. *J. Phys. Chem. A.* **113**, 2397–2404 (2009)
  19. S. Bale, N. Srinivas Rao, R. Syed, Effect of alkaline earths on spectroscopic and structural properties of  $\text{Cu}^{2+}$  ions-doped lithium. *Solid State Sci* **10**, 326 (2008)
  20. I. Ardelean, S. Cora, D. Rusu, EPR and FT-IR spectroscopic studies of  $\text{Bi}_2\text{O}_3-\text{B}_2\text{O}_3$  CuO glasses. *Phys. B* **403**, 3682–3685 (2008)
  21. H. Doweidar, Y.B. Saddeek, FTIR and ultrasonic investigations on modified bismuth borate glasses. *J. Non-Cryst. Solids.* **355**, 348–355 (2009)
  22. D. Saritha, Y. Markandeya, M. Salagram, M. Vithal, A. Singh, G. Bhikshamaiah, Physical and optical properties of  $\text{Bi}_2\text{O}_3-\text{B}_2\text{O}_3$  glasses. *J. Non-Cryst. Solids.* **354**, 5573–5579 (2008)
  23. Y.B. Saddeek, M.S. Gaafar, Properties of tellurite glass doped with ytterbium oxide for optical applications. *Mater. Chem. Phys.* **115**, 280–286 (2009)
  24. R.D. Husung, R.H. Doremus, The infrared transmission spectra of four silicate glasses before and after exposure to water. *J. Mater. Res.* **5**, 2209–2217 (1990). <https://doi.org/10.1557/JMR.1990.2209>
  25. N.F. Mot, E.A. Davis, *Electronic Processes in Non-crystalline Materials*, 2nd edn. (Oxford University Press, Oxford, 1979), p. 273
  26. A. Klonkowski, Bond characteristics of phosphate glasses of the M (II)  $\text{O}-\text{P}_2\text{O}_5$  type. I: The extreme position of strontium phosphate glasses. *Phys. Chem. Glasses.* **26**, 11–16 (1985)
  27. H. Aboud, H. Wagiran, R. Hussin, S. Saber, M.A. Saeed, Photoluminescence and thermoluminescence properties of  $\text{SnO}_2$  nanoparticles embedded in  $\text{Li}_2\text{O}-\text{K}_2\text{O}-\text{B}_2\text{O}_3$  with Cu-doping. *Chin. Opt. Lett.* **11**, 091603 (2013)
  28. V. Dimitrov, T. Komatsu, An interpretation of optical properties of oxides and oxide glasses in terms of the electronic ion polarizability and average single bond strength. *J. Univ. Chem. Technol. Metall.* **45**, 219–250 (2010)
  29. G.P. Singh, S. Kaur, P. Kaur, D.P. Singh, Modification in structural and optical properties of ZnO,  $\text{CeO}_2$  doped  $\text{Al}_2\text{O}_3-\text{PbO}-\text{B}_2\text{O}_3$  glasses. *Phys. B* **407**, 1250–1255 (2012)
  30. M.M. Ahmead, C.A. Hogarth, M.M. Khan, A study of the electrical and optical properties of The  $\text{GeO}_2-\text{TeO}_2$  glass system. *J. Mater. Sci. Lett.* **19**, 4040 (1984)
  31. V. Dimitrov, T. Komatshu, Classification of simple oxide: a polarizability approach. *J. Solid State Chem.* **163**, 100–112 (2002). <https://doi.org/10.1006/jssc.2001.9378>
  32. M. Abdal-Baki, F.A. Abdel-Wahab, A. Radi, F. El-Diasty, Factors affecting optical dispersion in borate glass systems. *J. Phys. Chem. Solids.* **68**(8), 1457–1470 (2007). <https://doi.org/10.1016/j.jpcs.2007.03.026>
  33. F. Nawas, M.R. Sahar, S.K. Ghoshal, R.J. Amjad, M.R. Dousti, A. Awang, Spectral investigation of  $\text{Sm}^{3+}/\text{Yb}^{3+}$ -co-doped sodium tellurite glass. *Chin. Opt. Lett.* **11**, 61605 (2013)
  34. J.E. Shelby, J. Ruller, Properties and structure of lithium germanate glasses. *Phys. Chem. Glasses* **28**, 262–268 (1987)
  35. K. Annapurna, S. Buddhudu, Characterization of fluorophosphates optical glasses. *J. Solid State Chem.* **93**, 454–460 (1991)

**Publisher's Note** Springer Nature remains neutral with regard to jurisdictional claims in published maps and institutional affiliations.